HIGH-RESOLUTION STEPPED FREQUENCY INVERSE SYNTHETIC APERTURE RADAR IMAGING USING TIME-FREQUENCY TRANSFORMS

A. V. Karakasiliotis*, G. Boultadakis*, A. D. Lazarov, and P. V. Frangos***

* National Technical University of Athens, School of Electrical and Computer Engineering,Division of Information Transmission Systems and Materials Technology,
Radar Systems and Remote Sensing Laboratory,9 Iroon Polytechniou Street, 15773 Zografou, Athens, Greece
E-mail: anastasiskarak@yahoo.gr, gboult_@hotmail.com, pfrangos@central.ntua.gr
** Burgas Free University,62 San Stefano Street, Burgas, Bulgaria
E-mail: lazarov@bfu.bg

Abstract

In this paper, a two-dimensional (2-D) inverse synthetic aperture radar (ISAR) return signal model, recently proposed for the interesting case of illuminating a moving target with stepped frequency (SF) modulated pulses, is employed to describe the scattering response of simulated air-craft targets. Moreover, we propose an ISAR imaging approach that consists of a cross-correlation algorithm for range compression and a linear or bilinear time-frequency (TF) transform for azimuth compression.

The proposed approach circumvents the motion compensation necessity through averaging of all image frames. Additionally, simulation results, for signal-to-noise ratio (SNR) of 20dB and target orientation angle of 40°, indicate that the most efficient TF transformations result in clear ISAR images and outperform the classical FFT based azimuth compression.

1. INTRODUCTION

In this paper, a two-dimensional (2-D) inverse synthetic aperture radar (ISAR) return signal model, recently proposed for the case of stepped frequency (SF) modulation [1], is exploited for realistic description of the scattering behaviour of the target to be imaged. Moreover, we propose an ISAR imaging approach that consists of a cross-correlation algorithm for range compression and a linear or bilinear time-frequency (TF) transform for azimuth compression.

The target to be imaged is represented by a rectangular grid of point scatterers, with the corresponding scattering intensities describing its geometrical shape. In contrast to the usual assumption in ISAR imaging, that of uniform rotational motion of the target around its mass-center, in this paper we assume that the target moves along a rectilinear trajectory at constant speed, without any rotational motion. Thus, the inverse synthetic aperture results from the translational motion of the target for a short period of time.

The cross-correlation based range compression technique [1] is applied to the synthetic 2-D raw data, which are generated via the employed 2-D SF ISAR return signal model. The resultant range profiles constitute the input data for the TF transform based azimuth compression technique. For each range cell, a time history series, with length equal to the number of SF bursts transmitted during the coherent processing interval, is transformed to a range and instantaneous Doppler image. Furthermore, time sampling leads to a reduced number of image frames, adequate to describe the time-varying Doppler frequency shift of each point scatterer of the target of interest. The final step of the proposed ISAR imaging approach is the integration of the retained image frames, which results in a superresolution range-Doppler image.

Conventional linear TF transforms, such as the short-time Fourier transform (STFT), and, more sophisticated bilinear TF transforms, such as the pseudo Wigner-Ville distribution (PWVD) and its smoothed version (SPWVD), are used in the present study. Low cross-term interference is a desirable feature for the bilinear transforms, which usually exhibit better resolution in both time and frequency than the linear transforms. In this paper, we examine the image focusing efficiency of each transform.

As a means of assessing the validity of the proposed ISAR imaging approach, numerical simulations are carried out for a particular SF ISAR scenario causing unfocusing in case of FFT based image formation, and high-resolution ISAR images are generated for a simulated Mirage 2000 aircraft geometry. Based on the visual examination of the obtained ISAR images, we conclude that the proposed imaging methodology is very efficient for realistic ISAR scenarios.

This paper is organized as follows. In Section 2, we briefly describe the employed 2-D SF ISAR return signal model. Section 3 includes the mathematical description of the proposed ISAR imaging approach. Section 4 presents the simulation results for the examined ISAR scenario, and, the performance of the applied TF transformations is evaluated in terms of ISAR image resolution and cross-term interference reduction. Finally, in Section 5, useful conclusions are drawn with respect to the present study.

2. 2-D ISAR RETURN SIGNAL MODEL

It is a common practice to consider the target to be imaged as an assembly of point scatterers or distributed scattering centers [2], an approach which is widely adopted for high radar frequencies. In this paper, we adopt for simplicity a point scatterer model.

Furthermore, we model the 2-D ISAR geometry with the object and the ISAR being placed in separate coordinate systems. Details with respect to the geometrical modelling can be found in [1].

An analytical geometrical model of the time-domain ISAR return signal for the case of SF modulation has been recently proposed [1], and its validity has been proven for realistic ISAR scenarios. In the present study, we employ this model as an ideal characterization of the point scattering behaviour of the target to be imaged.

For the SF ISAR functionality, a series of bursts of SF pulses is emitted. Here, we assume that each burst consists of M pulses, to which SF modulation is applied. Moreover, N bursts are transmitted during the coherent processing interval.

The overall ISAR return signal is the sum of the deterministic data component $S(p,m)$ and the random noise component $n(p,m)$, which is assumed to be white Gaussian. The following equations summarize the 2-D SF ISAR return signal model proposed and thoroughly described in [1].

$$S_n(p,m) = S(p,m) + n(p,m) \tag{1}$$

$$S(p,m) = \sum_{i=0}^{I-1}\sum_{j=0}^{J-1}\left\{\begin{array}{l} a_{ij}\cdot rect\left(\dfrac{t-t_{ij}(p)}{T_b}\right)\cdot \\ \cdot\exp\left[j\,2\pi\cdot f_{m-r+1}\cdot\left(t-t_{ij}(p)\right)\right]\end{array}\right\} \tag{2}$$

where

a_{ij} denotes the scattering intensity for the ij th point scatterer;

$t_{ij}(p) = \dfrac{2\cdot R_{ij}(p)}{c}$ is the round-trip delay of the ISAR signal backscattered from the ij th point scatterer, for the p th emitted burst;

$R_{ij}(p)$ denotes the magnitude of the distance vector from the ISAR to the ij th point scatterer of the target;

$t = t_{ij\min}(p) + (m-1)\cdot T$ is the dwell time of the ij th point scatterer;

T and T_b stand for the pulse and burst repetition intervals respectively;

$f_{m-r+1} = f_0 + (m-r)\cdot \Delta f$ is the received pulse frequency, appropriately indexed in order to take into account the reception time offset of the ISAR signal reflected from the ij th point scatterer, with respect to $t_{ij\min}(p)$;

Δf is the frequency step of the SF modulation.

In the above equations, p and m are the burst and sample indices respectively ($p=\overline{1,N}$, $m=\overline{1,M+L(p)}$, $L(p)=\left\lceil \frac{t_{ij\max}(p)-t_{ij\min}(p)}{T} \right\rceil$), while indices i, j determine a particular point scatterer on the target grid, whose size is $I \times J$.

3. PROPOSED ISAR IMAGING APPROACH

Range and azimuth compression are the fundamental procedures performed by a conventional radar receiver, in order to form a well-focused 2-D ISAR image.

3. 1. Cross-Correlation Based Range Compression

The cross-correlation based approach to range compression is realized by cross-correlating each burst of the received raw data $S_n(p,m)$ with a reference signal of the form $s_{ref}(m)=\exp\left[j2\pi f_m(m-1)T\right]$, $m=\overline{1,M}$, i.e. a SF burst starting to be transmitted at $t=0$. The result is one range profile for each received burst.

The cross-correlation based range compression is mathematically described by

$$\hat{S}(p,n_{ccl}) = \sum_{m=n_{ccl}}^{n_{ccl}+M-1} \left\{ \begin{array}{l} S_n(p,m)\cdot \\ \cdot\exp\left[-j2\pi f_{m-n_{ccl}+1}(m-n_{ccl})T\right] \end{array} \right\} \tag{3}$$

where $f_{m-n_{ccl}+1} = f_0 + (m-n_{ccl})\cdot \Delta f$ and $n_{ccl} = \overline{1, L_{\max}+1}$ ($L_{\max} = \max\{L(p)\}$) is the cross-correlation lag.

3. 2. Time-Frequency Transform Based Azimuth Compression

Our basic goal is the generation of a clear ISAR image of the moving target. In order to achieve this goal, a TF transform with superior resolution and low cross-term interference is needed. To apply the TF transform based image formation, we need a transform specially designed for computing time-varying spectrum and retrieving instantaneous Doppler frequency information. Having achieved a high-resolution time-varying Doppler spectrum, it is not necessary to flatten out the distribution of the radar frequency spectrum and to compensate for the individual motions of target's scatterers [3].

The range profiles, obtained by range compression of the received ISAR signal, constitute the input data for the TF transform based azimuth compression technique. For each range cell, a time history series, with length equal to the number of SF bursts, is transformed to a range and instantaneous Doppler image (image frame).

In our numerical experiments, an averaging of all image frames, produced from the TF transformation, is carried out to obtain a high-resolution ISAR (or range-Doppler) image.

3.2.1. Linear Transformation

One of the most known linear TF transforms is the Short Time Fourier Transform (STFT). STFT is based on the Fourier transform and its basic idea is the application of a moving time-domain window ($w(t)$). Mathematically expressed

$$\mathrm{STFT}(t,\omega) = \int s(t')w(t'-t)\exp(-j\omega t')dt' \tag{4}$$

In our simulations, a Hamming window is applied.

3.2.2. Bilinear Transformations

The most classical bilinear TF transform is the Wigner-Ville Distribution (WVD) [4]. In the WVD, the time-dependent autocorrelation function is given by the following equation.

$$\mathrm{WVD}(t,\omega) = \int s(t+\frac{t'}{2})s^*(t-\frac{t'}{2})\cdot\exp\{-j\omega t'\}dt' \tag{5}$$

Even though the usefulness of the WVD for signal processing purposes has been well recognized for a rather long period, its applications are limited mainly due to the "cross-term interference" problem.

In order to reduce the problem of cross-term interference, a wide variety of bilinear TF transforms has been proposed in the literature [3]. Of particular importance is the Cohen's class of bilinear TF transforms [5]. The TF distributions, according to Cohen, can be written in a more generalized form, each using a different two-dimensional kernel function called the "parameterization function".

A member of Cohen's class is the Pseudo Wigner-Ville Distribution (PWVD). Its mathematical definition is given in [6]

$$\mathrm{PWVD}(t,\omega) = \int \mathrm{h}(t')\mathrm{s}(t+t'/2)\mathrm{s}^{*}(t-t'/2)\mathrm{e}^{-\mathrm{j}\omega t'}\mathrm{d}t' \tag{6}$$

It is obvious that the PWVD is a windowed version of WVD. The new parameter $h(t')$ is a regular window, which typically results in frequency-domain smoothing of the WVD [6]. This means that the interference terms of the basic Wigner-Ville Distribution, because of their oscillatory nature, are attenuated in this new distribution. A Hamming time-domain window is used in our simulations.

By considering a separable smoothing function [6], we add a degree of freedom in the PWVD. This smoothing function is mathematically described by

$$\Pi(t,\omega) = \mathrm{g}(t)\mathrm{H}(-\omega) \tag{7}$$

where $H(\omega)$ is the Fourier transform of a smoothing window $h(t)$. In this way, we allow for independent control of the smoothing applied on the WVD, in both time and frequency. This becomes obvious in the following distribution

$$\mathrm{SPWVD}_{\mathrm{s}}^{(\mathrm{g},\mathrm{H})}(t,\omega) = \iint_{t'\omega'} \begin{array}{l} \mathrm{g}(t-t')\mathrm{H}(\omega-\omega')\cdot \\ \cdot \mathrm{W}_{\mathrm{s}}(t',\omega')\mathrm{d}t'\mathrm{d}\omega' \end{array} \tag{8}$$

which is known as the Smoothed Pseudo Wigner-Ville distribution (SPWVD) [5]. The SPWVD allows the smoothing spreads, Δt and $\Delta\omega$, to be adjusted independently. This

distribution is characterized by a separable smoothing kernel with two windows, whose effective lengths independently determine the time and frequency smoothing spread [5]. In our simulations, Hamming windows are used for time and frequency smoothing.

Furthermore, another important form of bilinear TF transformations is the Butterworth Distribution (BUD). Its parameterization function is defined as

$$\varphi_{\mathrm{BUD}}(\omega',t') = \frac{1}{1+\left(\frac{\omega'}{\omega'_1}\right)^{2N}+\left(\frac{t'}{t'_1}\right)^{2M}} \tag{9}$$

(N, M, $\omega'_1, t'_1 > 0$)

It acts as a 2-D low-pass filter with a variably flat passband and narrow transition region. Thus, it results in simultaneous reduction of the cross terms and preservation of the auto-terms [8]. Butterworth distribution is defined as

$$\mathrm{BUD}(t,\omega) = \frac{1}{2\pi}\iint \left\{ \begin{array}{l} \sum_{i=1}^{N} \alpha_i \left|\frac{t'_1}{t'}\right|^{M/N} \exp[-\beta_i \left|\frac{t'_1}{t'}\right|^{M/N} |t|]\cdot \\ \cdot\cos(\omega_1 \left|\frac{t'_1}{t'}\right|^{M/N} |t| - \psi_i)\cdot \\ \cdot s(u+\frac{t'}{2}) s^*(u-\frac{t'}{2}) \exp\{-j\omega t'\} du dt' \end{array} \right\} \tag{10}$$

4. SIMULATION RESULTS

In our numerical experiments, we have simulated the 2-D SF ISAR scenario with the specific parameters included in Table 1.

For all TF transforms, except for the STFT, averaging of all generated image frames is carried out and the resultant ISAR images are presented below (Figs. 1-6). The middle image frame is shown for the STFT case (Fig. 2).

Notice that the image focusing efficiency is significantly increased for the PWVD, the SPWVD and the BUD, compared to the conventional FFT technique.

Table 1. 2-D SF ISAR Scenario

Simulation Parameter	Parameter Value
aircraft type	Mirage 2000C
aircraft length	15.5 [m]
aircraft wingspan	8.5 [m]
target grid cell dimensions $\Delta X = \Delta Y$	0.5 [m]
"reference" point coordinates $\{ x_{00}(0),\ y_{00}(0) \}$	{0, 10} [Km]
vector velocity magnitude V	300 [m/sec]
vector velocity angle a	180 [°]
target orientation angle φ	40 [°]
initial carrier frequency f_0	10 [GHz]
square resolution $\Delta r_s = \Delta r_c$	0.5 [m]
radar bandwidth B	300 [MHz]
number of pulses M	64
frequency step Δf	4.6875 [MHz]
pulse repetition interval T	26.562 [μsec]
burst duration T_b	1.699 [msec]
number of bursts N	768

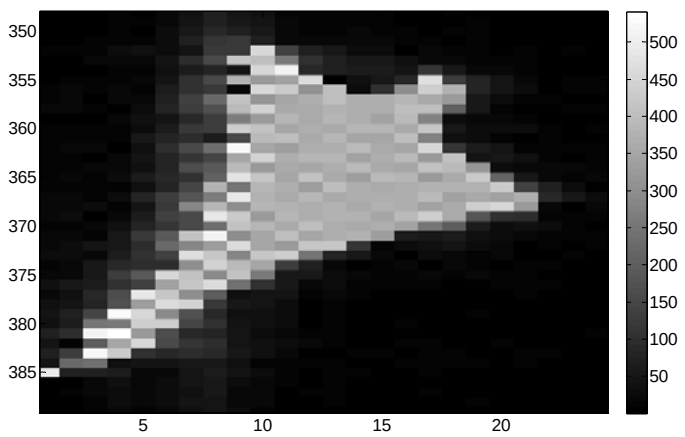

Figure 1. Reconstructed ISAR image via FFT based azimuth compression

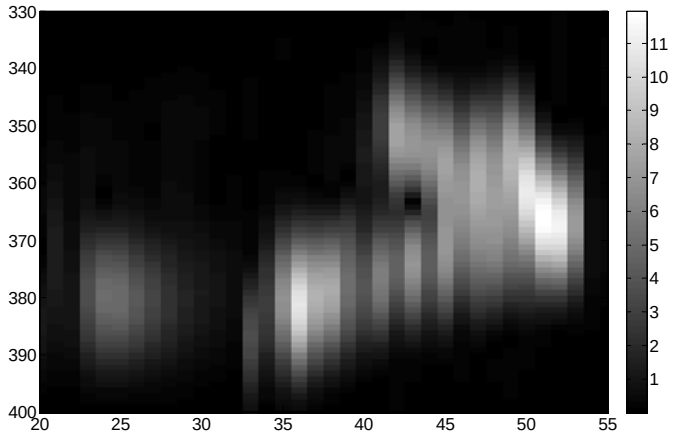

Figure 2. Reconstructed ISAR image via STFT based azimuth compression

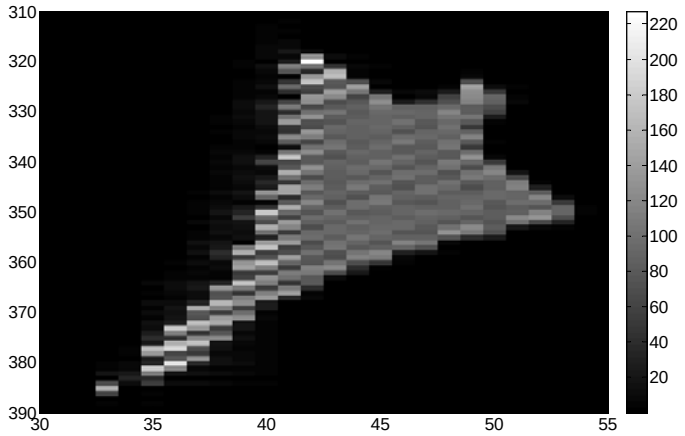

Figure 3. Reconstructed ISAR image via WVD based azimuth compression

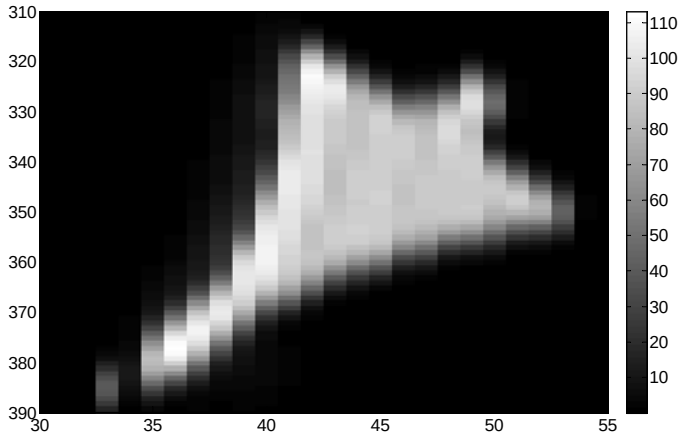

Figure 4. Reconstructed ISAR image via PWVD based azimuth compression

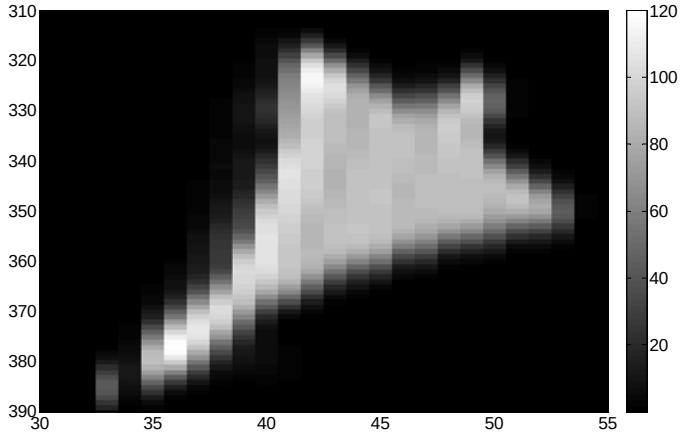

Figure 5. Reconstructed ISAR image via SPWVD based azimuth compression

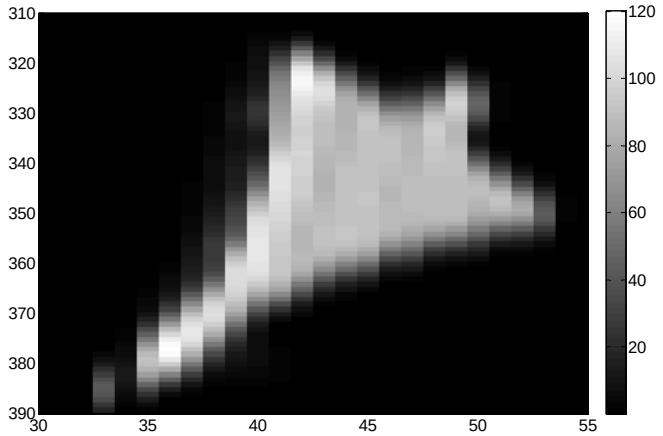

Figure 6. Reconstructed ISAR image via BUD based azimuth compression

5. CONCLUSIONS

In this paper, we have applied several TF transforms for realistic ISAR imaging. Bilinear transforms result in quite clear images, while circumventing the motion compensation necessity. For the simulated ISAR scenario, PWVD, SPWVD and BUD transformations have outperformed the classical FFT based azimuth compression.

REFERENCES

[1] A. Karakasiliotis, A. Lazarov, and P. Frangos, “Two-dimensional ISAR Model and Image Reconstruction with Stepped Frequency Modulated Signal,” *accepted for publication to IET Signal Proc.*, May 2008.

[2]M. Gerry, L. Potter, I. Gupta, and A. van der Merwe, “A Parametric Model for Synthetic Aperture Radar Measurements,” *IEEE Trans. Antennas Propag.*, July 1999, Vol. 47, no. 7, pp. 1179-1188.

[3]V. Chen, and H. Ling, Time-Frequency Transforms for Radar Imaging and Signal Analysis, Artech House, Boston-London, 2002.

[4]S. Qian, and D. Chen, “Decomposition of the Wigner-Ville Distribution and Time-Frequency Distribution Series,” *IEEE Trans. Signal Proc.*, Oct. 1994, Vol. 42, no. 10, pp. 2836-2842.

[5]F. Hlawatsch, and G. F. Boudreaux-Bartels, “Linear and Quadratic Time-Frequency Signal Representations,” *IEEE Signal Proc. Mag.*, Apr. 1992, pp. 21-67.

[6]F. Auger, P. Flandrin, P. Goncalves, and O. Lemoine, “Time-Frequency Toolbox for Use with MATLAB (tutorial),” July 1997.

[7]H. Choi, and W. Williams, “Improved Time-Frequency Representation of Multi-component Signals using Exponential Kernels,” *IEEE Trans. Acoust. Speech and Signal Proc.*, June 1989, Vol. 37, no. 6, pp. 862-871.

[8]A. Papandreou, and G. F. Boudreaux-Bartels, “Generalization of the Choi-Williams Distribution and the Butterworth Distribution for Time-Frequency Analysis,” *IEEE Trans. Signal Proc.*, Jan. 1993, Vol. 41, no. 1, pp. 463-472.